doi:10.3788/gzxb20164502.0224003

一种石墨烯波导褶皱激发表面等离子体激元的设计

朱君[a],秦柳丽[b],傅得立[a],宋树祥[a]
(广西师范大学 a.电子工程学院;b.数学与统计学院,广西 桂林 541004)

摘 要:设计了褶皱石墨烯波导结构激发表面等离子体激元,通过设计周期阵列结构实现了表面等离子体激元传播损耗的补偿.理论分析了周期阵列结构的表面等离子体激元传播模型和补偿损耗的方式,结果表明褶皱衍射激发表面等离子体激元波导不仅能够激发表面等离子体激元,还能利用表面等离子体激元波矢关系实现器件参数控制,周期阵列增益全程补偿损耗的方式可以显著增加表面等离子体激元的传播距离.数值分析结果进一步表明:该结构具备了保持亚波长尺寸的强局域化优势;周期阵列增益全程补偿可以显著提高纳米腔中的电场强度,降低传输损耗;波导结构的粒子反转水平较高,自发辐射噪声的扰动较低.设计的石墨烯波导器件可以为微纳光学集成、光子传感和测量等领域提供理想的亚波长光子器件.

关键词:亚波长光学;表面等离子体激元;周期褶皱结构;周期阵列结构;纳米腔
中图分类号:TB383.1 **文献标识码**:A **文章编号**:1004-4213(2016)02-0224003-6

Design of Folds Graphene Waveguide Excited Surface Plasmon Polaritons

ZHU Jun[a], QIN Liu-li[b], FU De-li[a], SONG Shu-xiang[a]
(a. *College of Electronic Engineering*; b. *College of Mathematics and Statistics*, *Guangxi Normal University*, *Guilin*, *Guangxi* 541004, *China*)

Abstract: The folds graphene waveguide excited Surface Plasmon Polaritons(SPPs) was designed and full compensation structures could be realized with periodic array by graphene material. The propagation model of period folds excited SPPs and the full compensation were analyzed theoretically. The results of theoretically analysis show that the period fold structure can not only excite SPPs, but also control device parameters using SPPs wave relations. In addition, periodic array compensation can significantly increase the propagation distance of SPPs. Further simulation results show that the proposed structure has the advantage of strong localized and subwavelength waveguide size; periodic array compensation can significantly improve the electric field strength of nanocavity; structure of graphene waveguide expresses high levels of population inversion and low spontaneous emission noise disturbance. The proposed graphene waveguide devices can be provided for the micro-nano optics, photonic sensing and measurement.

Key words: Subwavelength optics; Surface plasmon polaritons; Cycle fold structure; Periodic array structure; Nano-cavities
OCIS Codes: 240.6680; 160.3918; 140.3948; 160.4236

0 Introduction

Optical interconnects possess an unimaginable data carrying capacity, which may allow photonic components to mitigate the present bottlenecking in increasing the computational speed. However, their

Foundation item: The National Natural Science Foundation of China (No. 61361011), Guangxi Natural Science Foundation (No. 2015GXNSFBA139257), Guangxi Normal University Doctor Scientific Research Foundation, Guangxi Normal University Key Program (No. 2015ZD03)
First author: ZHU Jun(1985—), male, lecturer. Ph. D. degree, mainly focuses on directions for nonlinear optics, surface plasma science research areas. Email: zhujun1985@mailbox.gxnu.edu.cn
Received: Aug. 24, 2015; **Accepted**: Oct. 08, 2015

implementation is hindered by the physical size or dimensional mismatch between electronic and dielectric photonic components[1-2]. Moreover it is expected that Complementary Metal Oxide Semiconductor (CMOS) foundries will further decrease the feature sizes on silicon chips[3], ultimately down to 10 nm. Such reduction in size would further increase the dimensional mismatch between the electronic and optical elements, as the size of the dielectric photonic devices is restricted by the diffraction limit[4-5]. Moreover, miniaturization introduces several problems including dielectric break down, hot carriers and short channel effects, that degrade device reliability[6]. The Surface Plasmon Polaritons (SPPs), spatially confined Transverse Magnetic (TM) electromagnetic modes propagating at the metal-dielectric interfaces, offer the bandwidths of photonic devices and physical dimensions shared with nanoscale electronics. The potential of plasmonics to bridge the gap between electronics and photonics is now well recognized by the scientific community with a large number of investigators working in the field of plasmonics[7-8]. Nikolajsen team of Denmark used thermo-optic effect on the strip of metal embedded in polymer materials to achieve light modulator and optical switches, and the transmission loss of 20nm thick gold-plate waveguide is as low as 6 dB/cm in optical communication wavelength window. However, this model of the waveguide size has gone up to 12 μm[9]. The cooperation project of Zhejiang University and Sweden's Royal Institute of Alfven Laboratory group put forward the SPPs waveguide of metal slot. They undertook an in-depth theoretical of optical modes. Also the team get that waveguide of subwavelength scale can be achieved limits of optical field, which is loss up to 4 dB/μm. At the same time, Bozhevolnyi team from Aalborg University, Denmark, used focused-ion beam etching process and near-field scanning optical microscopy to study v-groove SPPs waveguide devices[10]. They used conformation to wavelength division multiplexers, which is Bragg grating filters based on Metal Insulator Metal (MIM) structure. They simultaneously achieved the filtering of applications for SPPs wave[11]. In 2007, the cooperated research team by State Key Laboratory of superconducting physics and optical physics studied the periodic hole arrays in metallic films. They get higher order surface plasmon resonance peaks at the first time[12], and enhanced of electric field was the diffraction of SPPs based on theoretical analysis of Maxwell equations. The team by CAs semiconductor Nano-Photonics Laboratory and Hebei Polytechnic University get vertical-cavity surface-emitting lasers in normal 850nm, which achieved diameter of small holes by 100nm and 400nm respectively, and the output power is up to 0.5nW[13]. With the deepening of the study, researchers have found that it was difficult to control the permittivity of medium and the loss of metal, which was especially in the visible band[14-15]. Meanwhile, graphene materials became the current focus of research directions[16], which is very suitable for optical device application. Particularly graphene is applied to SPPs propagation that the loss is obviously less than precious metals, such as gold, silver, etc[17-18]. In particular, in 2012 the scientists from the United States University of California at San Diego, published the surface of graphene excites the electron wave by infra-red light beam by Nature. And they can through a simple circuit to control the wave length and height of surface plasmon oscillation[19]. Based on above development background, we design graphene waveguide of SPPs. And we design folds structure to achieved SPPs excited. The array column structure of graphene waveguide can compensation SPPs loss. Theory analysis and simulation results showed that the structure can keep subwavelength confined while the distance of SPPs was enhanced.

1 Design of structure

In order to achieve the loss compensation of SPPs propagation, the structure shown in Fig. 1 is used widely. Increasing the gain medium of Fig. 1 is a method to compensate the loss, but this approach has only theoretical feasibility. Recently researchers discover that the structure of Fig. 1 is difficult to apply in the waveguide of dimension microelectronic integrated and photonic circuit

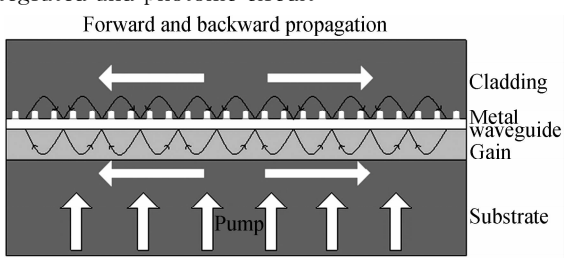

Fig. 1 Typical SPPs loss compensation

We use Insulator Metal Insulator (IMI) waveguide structure to optimize the above problems. Also we consider saturated absorber and organic dye hybrid is implanted which is compensated for the loss of SPPs. The compensation structure is shown in Fig. 2. The structure shows that when SPPs go through the saturated absorber, it will produce a corresponding fast zoom mode. Then the number of surface plasma waves is increased, it is also reduced the spontaneous emission noise that caused in this process.

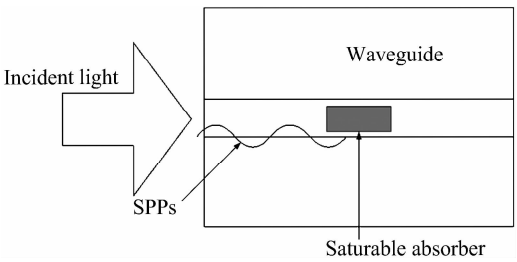

Fig. 2 Saturable absorber implants

The particular design of the structure is shown in Fig. 3. The incident light source go into folded structure of graphene waveguide, which is excited SPPs. Then SPPs propagate through the array dye of the gain medium that can compensate the loss. The length of structure is 4200nm, the width is 2 700 nm, and the 900 nm thick Si substrate grow on the SiO_2 800 nm thick in an oxygen environment. After that, we use the method of electron beam reticle to get a depth of 600 nm graphene waveguides. In the graphene waveguides, we use the plasma dry method to etch fold structure which with the length of 1 200 nm and the period of 200 nm. At the SiO_2 layer, we use the plasma dry method to etch the growth cycle of 2 200 nm and the period of 400 nm gain medium tank. We use spinning method to fill an array of gain compensation medium. The gain medium is the hybrid of rhodamine dye indole pentamethine saturated absorber dyes, and the premixed ratio of the number of molecules is 2 : 1. Finally we use ultraviolet lights to dry, which can control the gain medium. Due to the structure by the graphene low loss and good conductor characteristics, it can overcome the noise generated by spontaneous emission channel. The whole array dye gain loss compensation has a good adaptability to wavelength, and a high quantum efficiency. The use of array full compensation can significantly increase the SPPs propagation distance.

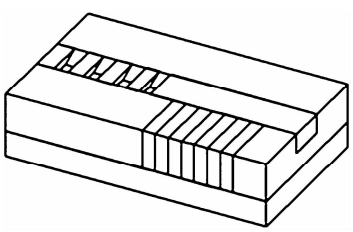

Fig. 3 Design of the structure

2 Analysis theory of structural

2.1 The excited SPPs mode of found structure

For the TM mode of subwavelength, the characteristic impedance can be defined as

$$Z=\frac{E_1 d}{H_2 w}=\frac{kd}{\varepsilon_1 w\omega} \tag{1}$$

where is incident light frequency, k is the propagation constant of TM mode. w, d are the width of x_2, x_3 direction of waveguide respectively. Characteristic impedance is reduced by reducing the waveguide width of the insulating layer, we also can fill higher refractive index into the insulating layer. Dispersion of characteristic impedance Z is small, especially in the larger wavelength region. When two waveguides having different characteristic impedance are connected, there is reflection at its joints. Reflection can be reduced by match their impedance. When the width of the waveguide is much smaller than the wavelength, the transmission waveguide problem may be approximated to the transmission line model. The electromagnetic field of the junction of the waveguide transmission problems may correspond to the equivalent current and the equivalent voltage problems between the transmission lines. The voltage transmission line connections should be equal as

$$V_1^+ + V_1^- = V_2^+ + V_2^- \tag{2}$$

The equivalent current of the incident wave and the exit wave is equal to the sum of the equivalent current

$$I_1^+ + I_2^+ = I_1^- + I_2^- \tag{3}$$

Relation matrix of input equivalent voltage and out equivalent voltage is

$$\begin{bmatrix} V_1^- \\ V_2^- \end{bmatrix} = \begin{bmatrix} S_{11} & S_{12} \\ S_{21} & S_{22} \end{bmatrix} \begin{bmatrix} V_1^+ \\ V_2^+ \end{bmatrix} \tag{4}$$

where

$$\begin{aligned} S_{11} &= \frac{Z_2 - Z_1}{Z_1 + Z_2} \quad S_{12} = \frac{2Z_1}{Z_1 + Z_2} \\ S_{21} &= \frac{2Z_2}{Z_1 + Z_2} \quad S_{22} = \frac{Z_1 - Z_2}{Z_1 + Z_2} \end{aligned} \tag{5}$$

There is only one reflection at the signal interface between the two waveguide, and if the two different waveguides alternately laminated to form a periodic structure, the plurality of waveguide reflection at the interface is possible to greatly improve the superposition total energy reflectivity. We consider that a periodic waveguide structure with different width of the waveguides A and B connected, their width are d_A and respectively, and their length are and l_B, respectively. Equivalent voltage of the n-th cycle units may be written as

$$V_n^A = V_n^{A+} e^{-ik_A x_1} + V_n^{A-} e^{ik_A x_1} \tag{6}$$

$$V_n^B = V_n^{B+} e^{-ik_B x_1} + V_n^{B-} e^{ik_B x_1} \tag{7}$$

where $+-$ represent positive and negative direction of x_1 axis. They can be written in the form of the transfer matrix

$$\begin{bmatrix} V_n^+ \\ V_n^- \end{bmatrix} = \boldsymbol{D}_{AB}\boldsymbol{P}_B\boldsymbol{D}_{BA}\boldsymbol{P}_A \begin{bmatrix} V_{n+1}^- \\ V_{n+1}^+ \end{bmatrix}$$

$$\boldsymbol{D}_{AB} = \begin{bmatrix} \frac{1}{2}(1+\frac{Z_A}{Z_B}) & \frac{1}{2}(1-\frac{Z_A}{Z_B}) \\ \frac{1}{2}(1-\frac{Z_A}{Z_B}) & \frac{1}{2}(1+\frac{Z_A}{Z_B}) \end{bmatrix}$$

$$\boldsymbol{D}_{\mathrm{BA}}=\begin{bmatrix}\frac{1}{2}(1+\frac{Z_{\mathrm{B}}}{Z_{\mathrm{A}}}) & \frac{1}{2}(1-\frac{Z_{\mathrm{B}}}{Z_{\mathrm{A}}})\\ \frac{1}{2}(1-\frac{Z_{\mathrm{B}}}{Z_{\mathrm{A}}}) & \frac{1}{2}(1+\frac{Z_{\mathrm{B}}}{Z_{\mathrm{A}}})\end{bmatrix}$$

$$\boldsymbol{P}_{\mathrm{A}}=\begin{bmatrix}\mathrm{e}^{\mathrm{i}k_{\mathrm{A}}l_{\mathrm{A}}} & 0\\ 0 & \mathrm{e}^{-\mathrm{i}k_{\mathrm{A}}l_{\mathrm{A}}}\end{bmatrix}$$

$$\boldsymbol{P}_{\mathrm{B}}=\begin{bmatrix}\mathrm{e}^{\mathrm{i}k_{\mathrm{B}}l_{\mathrm{B}}} & 0\\ 0 & \mathrm{e}^{-\mathrm{i}k_{\mathrm{B}}l_{\mathrm{B}}}\end{bmatrix}$$

$$\boldsymbol{M}=\boldsymbol{D}_{\mathrm{AB}}\boldsymbol{P}_{\mathrm{B}}\boldsymbol{D}_{\mathrm{BA}}\boldsymbol{P}_{\mathrm{A}}=\begin{bmatrix}m_{11} & m_{12}\\ m_{21} & m_{22}\end{bmatrix} \tag{8}$$

For the period structure with N basic units, the transfer matrix can be expressed as

$$\begin{bmatrix}m_{11} & m_{12}\\ m_{21} & m_{22}\end{bmatrix}^{N}=$$

$$\begin{bmatrix}m_{11}U_{N-1}(\chi)-U_{N-2}(\chi) & m_{12}U_{N-1}(\chi)\\ m_{21} & m_{22}U_{N-1}(\chi)-U_{N-2}(\chi)\end{bmatrix} \tag{9}$$

where $U_N(\chi)$ is Chebyshev polynomial

$$U_N(\chi)=\frac{\sin\,(N+1)K\Lambda}{\sin\,K\Lambda} \tag{10}$$

where $\Lambda=l_A+l_B$ is the period of structure, K is Bloch vector

$$K=\frac{1}{\Lambda}\arccos\left(\frac{m_{11}+m_{22}}{2}\right) \tag{11}$$

When Bloch wave vector K is a real number, Bloch corresponding to the waveguide can transmit, Bloch wave vector K has an imaginary part, the transmission spectrum in the band gap. Incident electromagnetic wave produces a total reflection in the surface of the fold structure and the media, and there is a part of Contin evanescent wave tunneling into the media near to fully reflecting surface. The size of wave vector k_x is same as total reflection of electromagnetic waves, which is to say the incident electromagnetic wave excites evanescent wave propagating along the x direction in the graphene layers produced. The wave number of evanescent wave satisfies $k_x=k_0\sin\theta\pm nk_g$, where $k_g=2\pi/\lambda_g$, n is an integer.

2.2 The complete compensation analysis of array gain

One side of Branch waveguide is closed, and the other end is vertical to the main waveguide . A single branch structure is shown in Fig. 4. After the electromagnetic waves incident from the main waveguide, it goes through branch waveguide section. Due to the structure of non-continuity here, part of the energy is reflected and the other part into the support section or directly goes through the waveguide.

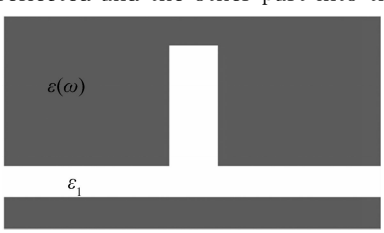

Fig. 4 Single stub structure

Here the transmission line uses a simplified model to analyze electromagnetic properties of the transmission branch section structure, so that the imaginary part of the complex permittivity of graphene is zero. The characteristic impedance of the main branch waveguide and waveguide sections, respectively, the transmission matrix is

$$\boldsymbol{M}=\begin{bmatrix}m_{11} & m_{12}\\ m_{21} & m_{22}\end{bmatrix}=\begin{bmatrix}1+\frac{Z_1}{2Z_2} & \frac{Z_1}{2Z_2}\\ -\frac{Z_1}{2Z_2} & 1-\frac{Z_1}{2Z_2}\end{bmatrix} \tag{12}$$

The energy reflectance and the transmittance nodules structure are respectively

$$\begin{aligned}R&=\left|\frac{m_{21}}{m_{11}}\right|^2=(\frac{Z_1}{2Z_2+Z_1})^2\\ T&=\left|\frac{1}{m_{11}}\right|^2=(\frac{2Z_2}{2Z_2+Z_1})^2\end{aligned} \tag{13}$$

Simplified expression stub impedance is

$$Z_2=\mathrm{i}Z_1\,\mathrm{ctg}(k_{\mathrm{sp}2}L) \tag{14}$$

where L is the depth of the support section $k_{\mathrm{sp}2}$ is the surface plasmon wave vector transfer of the support section . The waveguide transmission condition for 0 is

$$k_{\mathrm{sp}2}L=(m+\frac{1}{2})\pi \tag{15}$$

where m is non-negative integer. The nature of the support section of the waveguide structure can be used as a filter. Fig. 5 shows the periodic nodules compensation structure, the separation distance between two adjacent support sections is h, nodules width is d. Periodic branch section structure can be used to deal with the transmission line model, each basic cell comprises a length h of the main waveguide and a section of length L of the branched waveguide.

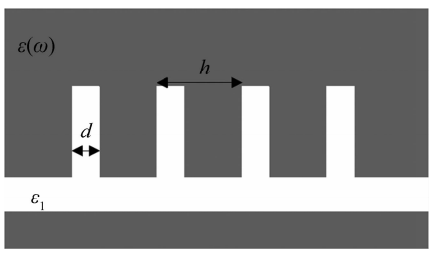

Fig. 5 Periodic stub structure

For the n-th cycle, the transfer matrix is expressed as

$$\begin{bmatrix}V_n^+\\ V_n^-\end{bmatrix}=\boldsymbol{M}_{n,n+1}\begin{bmatrix}V_{n+1}^+\\ V_{n+1}^-\end{bmatrix}$$

where,

$$\boldsymbol{M}_{n,n+1}=$$

$$\begin{bmatrix}m_{11} & m_{12}\\ m_{21} & m_{22}\end{bmatrix}=\begin{bmatrix}\mathrm{e}^{\mathrm{i}kh}[1+\frac{\mathrm{i}}{2}\mathrm{tg}(kl)] & \frac{\mathrm{i}}{2}\mathrm{tg}(kl)\\ -\frac{\mathrm{i}}{2}\mathrm{tg}(kl) & \mathrm{e}^{\mathrm{i}kh}[1-\frac{\mathrm{i}}{2}\mathrm{tg}(kl)]\end{bmatrix} \tag{16}$$

The Bloch equation is derived by use of Eqs. (15) and (16) as

$$\cos(Kh)=\cos(kh)-\frac{1}{2}\mathrm{tg}(kL)\sin(kh) \tag{17}$$

Since $K=\alpha+\mathrm{i}\beta$, and the right of Eq. (17) is a real number, $\beta=0$ or $\alpha h$is an integer multiple of π. The latter means that the electromagnetic wave can not be totally reflected. The forbidden band equation of this structure can be show as

$$\cosh(\beta h)=\left|\cos(kh)-\frac{1}{2}\mathrm{tg}(kL)\sin(kh)\right|>1 \tag{18}$$

Then, we can get

$$T=\frac{4}{4+\dfrac{\mathrm{tg}^2(kL)\sin^2(NKh)}{\sin^2(Kh)}} \tag{19}$$

The designed periodic waveguide may constitute the nano cavity. When the length of nano cavity matches with the forbidden band on both sides of the periodic structure, a defect mode can be got. The wavelength of defect mode is in the band gap of the periodic structure, but it can spread through the nano-cavities, the nature is same as Fabry-Perot (FP) cavity. Nano-cavity mold defected in the internal field distribution has a standing character, which can compensate for the loss SPPs waves.

3 Simulation analysis

3.1 The effect analysis of localization

As shown in Fig. 6, the structure was analyzed by Finite-Different Time-Domain (FDTD) strong localization effect. It can be seen from the Fig. 6 that the magnetic field of the waveguide structure has a good restriction. It can also be seen the field distribution is very strong in the top corner of the waveguide, which is due to the apex angle effect of the waveguide. There is a large number of bound charges in the corner area, it can produce oscillation shock, which makes the original field strength improved. The results show that the waveguide structure can not change the localization properties of SPPs, and the device structure is feasible.

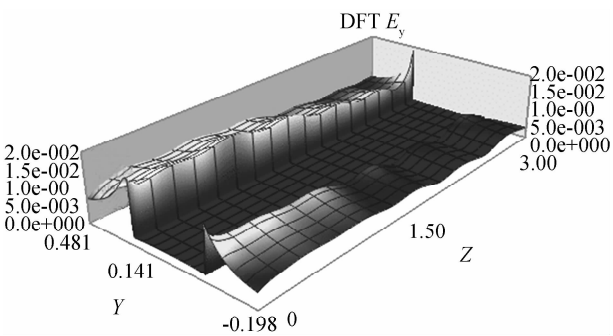

Fig. 6 The result of FDTD analysis

3.2 The effect analysis of gain compensation

Fig. 7 shows the transport properties by using the FDTD method to simulate the structure in different frequencies. In the simulation, waveguide width is 500 nm, two nodules are symmetrically distributed on both sides of the cavity structure, nodules depth is 474 nm, and the cavity length is 1 900 nm. The light wavelengths are 581.1 nm and 669.6 nm. Simulation results show the FP cavity transmission characteristics of nano-cavity structure. The light in the cavity resonance close to the transmission wavelength can continue through the nano-cavity, which is away from the resonance wavelength. Near field distribution of resonance wavelength is shown in Fig. 7(a), due to the transmission loss in the vicinity of 580 nm is very strong (the propagation length is about 6 μm), the electric field strength in the cavity is not greater than the value of the incident, but the transmission is stronger than the no nano cavity. If there is gain medium, there will be a greater increase in intracavity field. The resonance wavelength near field distribution is more media into the cavity section, which reduces the transmission loss.

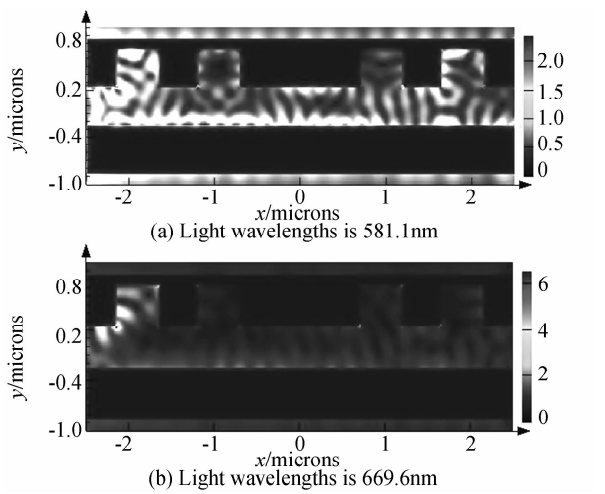

Fig. 7 Electric field distribution of nano-cavities on different frequencies

Consider a periodic defected support structures with width of d, the depth of nodules is $L=k(m+1/2\pi)$, nodules spacing is $h=km'\pi$, the support section of the structure shows strong reflection for a specific wavelength of SPPs. FDTD analysis shows that when the periodic structure defects stub length meets FP resonance conditions, it can become nano equivalent waveguide cavity structure.

Additionally, simulation studies show that only the change of geometry has an effect on eigenmode function, SPPs excitation curve is free from geometry factors. In particular the excitation curve of different SPPs with different depth waveguide completely overlap curve. The geometric characteristics of the system are fully described by the eigenmode function. Their nature entirely depends on the material

parameters.

4 Conclusion

The method of the whole array dye gain loss has a wavelength adaptability to organic dyes gain medium, and a high quantum efficiency. Full array compensation can significantly increase the SPPs propagation distance. The SPPs structure of graphene waveguide may be an ideal subwavelength photonic device for micro/nano integrated optics, photonics sensing and measurement provide, preparation techniques, which achieves a low cost. The proposed graphene waveguide devices can be provided for the micro-nano optics, photonic sensing and measurement.

Reference

[1] ALBUQUERQUE E L, COTTAM M G. Damping of surface plasmon - polaritons in semiconductor superlattices [J]. *Physica Status Solidi*, 1992, **170**(1):K17-K20.

[2] SHENG J S, LUE J T. Resonant reflectance dips induced by coupled surface plasmon polaritons in thin metal[J]. *Applied Physics A*, 1992, **55**(6):537-544.

[3] OKAMOTO T, HARAGUCHI M, FUKUI M. Optical bistability associated with surface plasmon polariton excitation [J]. *Journal of the Physical Society of Japan*, 1992, **61**(5): 1549-1555.

[4] KRENN R J, WEEBER C J. Surface plasmon polaritons in metal stripes and wires [J]. *Philosophical Transactions. Series A, Mathematical, Physical, and Engineering Sciences*, 2004, (1817):739-756.

[5] ZHONG Dong-zhou, JI Yong-qiang. Electro-optical composite logic gates based on periodically poled lithium niobate crystal [J]. *Acta Photonica Sinica*, 2015, **44**(5): 0523004

[6] ZHU Jun, LI Zhi-quan. Transmission characteristics of surface plasmon polariton based on strip structure[J]. *Acta Photonica Sinica*, 2014, **43**(10): 1005003

[7] LI Zhi-quan, YAN Lei, GUO Jia-liang, *et al*. Characteristic analysis of noise factor in the periodic stripe long range surface plasmon polaritons structure [J]. *Acta Photonica Sinica*, 2015, **44**(3): 0319001

[8] ABRAMOV A S, ZOLOTOVSKII I O, SEMENTSOV D I. Amplification of surface plasmon polaritons in the HTSC film - dielectric structure[J]. *Optics & Spectroscopy*, 2015, **119**(5):875-882.

[9] LIANG X, WANG J, TANG B, *et al*. Undirectional launcher of surface plasmon polaritons based on subwavelength slits with side-illumination and backside-illumination[J]. *Optik - International Journal for Light and Electron Optics*, 2016, **127**(3):1139 - 1143.

[10] HUANG Y, QIU W, LIN S, *et al*. Analysis of mode characteristics and output efficiency of graphene equilateral triangle nanocavity with vertex output waveguide[J]. *Optical & Quantum Electronics*, 2016, **48**(1):1-10.

[11] VJAHNG J, LADANI F T, KHAN R M, *et al*. Visualizing surface plasmon polaritons by their gradient force. [J]. *Optics Letters*, 2015, **40**(21):5058-5061.

[12] EVSEEV D A, SANNIKOV D G, SEMENTSOV D I. Surface plasmon polaritons at the interface between dielectric and anisotropic nanocomposite [J]. *Journal of Communications Technology & Electronics*, 2015, **60**(2): 158-165.

[13] JAHNG J, LADANI F T, KHAN R M, *et al*. Visualizing surface plasmon polaritons by their gradient force. [J]. *Optics Letters*, 2015, **40**(21):5058-5061

[14] GAO W, SHI G, JIN Z, *et al*. Excitation and active control of propagating surface plasmon polaritons in graphene[J]. *Nano Letters*, 2013, **13**(8):3698-3702.

[15] SALIHOGLU O, BALCI S, KOCABAS C. Plasmon-polaritons on graphene-metal surface and their use in biosensors[J]. *Applied Physics Letters*, 2012, **100**(21): 213110.

[16] BLUDOV Y V, FERREIRA A, PERES N M R, *et al*. A primer on surface plasmon-polaritons in graphene [J]. *International Journal of Modern Physics B*, 2013, **27**(10): 1-6.

[17] PERES N M R, YU V B, AIRES F, *et al*. Exact solution for square-wave grating covered with graphene: surface plasmon-polaritons in the terahertz range. [J]. *Journal of Physics. Condensed Matter : an Institute of Physics Journal*, 2013, **25**(12):269-275.

[18] ALDO A, COSTANTINO D A, ANDREA L, *et al*. Tuning of surface plasmon polaritons beat length in graphene directional couplers. [J]. *Optics Letters*, 2013, **38**(20):4228-4231.

[19] GAO Li-bo, REN Wen-cai, XU Hui-long, *et al*. Repeated growth and bubbling transfer of graphene with millimetre-size single-crystal grains using platinum [J]. *Nature Communications* 2012, **699**(3): 1-7.